J. Electrochem. Sci. Eng. **10(4)** (2020) 385-398; http://dx.doi.org/10.5599/jese.807

Open Access: ISSN 1847-9286
https://pub.iapchem.org/ojs/index.php/JESE

Original scientific paper

Pencil graphite electrodes as bioanodes for enzymatic glucose biofuel cell

Madhavi Bandapati[1], Sanket Goel[2] and Balaji Krishnamurthy[1,✉]

[1]*Department of Chemical Engineering, Birla Institute of Technology and Science (BITS) Pilani, Hyderabad Campus, Hyderabad, India*
[2]*MEMS and Microfluidics Lab, Department of Electrical and Electronics Engineering, Birla Institute of Technology and Science (BITS) Pilani, Hyderabad Campus, Hyderabad, India*

Corresponding author: ✉balaji@hyderabad.bits-pilani.ac.in, balaji.krishb1@gmail.com

Received: March 9, 2020; Revised: May 19, 2020; Accepted: May 26, 2020

Abstract

*This study investigates the performance of pencil graphite (PG) electrodes to identify the grade of pencil most suitable as bioanode for enzymatic glucose biofuel cell. Pencils of H, **3**H, **5**H and B grades are selected for this study. The surfaces of different grade PGs are modified with carboxylic acid functionalized multi walled carbon nanotubes (COOH-MWCNT/PG), followed by immobilization with glucose oxidase (GOx) to fabricate the respecttive bioanodes (GOx/COOH-MWCNT/PG). Morphological and electrochemical characterizations are carried out using scanning electron microscopy, electrochemical impedance spectroscopy, cyclic voltammetry and energy dispersive X-ray spectroscopy. All tested PG electrodes exhibited positive results with variable response characteristics towards glucose oxidation reaction. B-grade PG bioanode is found to have the highest coverage of the deposited nanobiocomposite with the fastest electron transfer rate. The half-cell electrode assembly with this grade of PG recorded the highest current density of 4.25 mA cm^{-2} at physiological glucose conditions (5 mM glucose, pH 7.0). Enzymatic glucose biofuel cell assembled with B-grade PG bioanode and platinum cathode generated an open circuit potential of 149 mV and maximum power density of 0.789 µW cm^{-2} from 5 mM glucose at ambient conditions (25 ± 3°C). The results obtained for B-grade PG bioanode are comparable to those of conventional carbon and glassy carbon electrodes, thus demonstrating its applicability to enzymatic glucose biofuel cells.*

Keywords

Pencil graphite electrode; bioanode; glucose oxidase; multiwalled carbon nanotubes; enzymatic glucose biofuel cell.

Introduction

Enzymatic glucose biofuel cells (EGBFCs) employ enzymes as catalysts which exhibit extremely specific electro-catalytic activities for biochemical and biological reactions [1]. These enzymes have relatively short life-span and redox centers are often buried deep inside the protein/glycoprotein shell, requiring thus pragmatic selection of electrode materials and fabrication of electrodes [2]. To establish efficient electron transfer between enzyme active sites and electrode, the enzyme must be supported with appropriate solid support, *i.e*. conducting support matrix, with adequate materials for binding and encapsulation, and with transport mediators [3]. To maximize the current output of the enzymatic redox reactions, a variety of materials are being explored as electrode substrates, including functionalized/conductive electroactive polymers, biocompatible composites, composites of organometallic compounds and transition metal-based complexes, hydro-gel and sol–gel materials, nanomaterials such as nano-metal oxides and composites [4,5].

Among low cost electrode substrates, pencil graphite (PG) electrodes have already established an active area of research. Aoki *et al*. have reported that the nature of PG influences the voltammetric and electroanalytical response of the analyte [6]. David *et al*. showed that just like other carbon-based working electrodes, PG presents high chemical and mechanical stability and large working potential window (-0.8 V to 0.6 V *vs*. SCE in acidic and alkaline solutions) [7]. Karuiki *et al.* have shown that the electron transfer rate of HB grade PG is similar to glassy carbon electrode [8]. Tavare *et al.* have found out that most PGs have electrical resistance less than 5 Ω and hence could be considered as electrode materials [9].

Typically, PG comprises clay and graphite. Increasing graphite content increases softness of pencil, while increasing the clay content adds hardness [10]. Accordingly, different grades of PG ranging from 8B (softest) to 9H (hardest), have already been studied for various electroanalytical applications [11,12]. Among different grade PGs (HB, H, F, 2H, 4H and 6H), Wang *et al.* have shown that HB grade pencil generated the most favorable response for stripping voltammetric analysis of RNA. The authors have also shown that 6H pencil displays the most favorable signal to background ratio in the electrochemical detection of deoxyribonucleic acid (DNA) [13,14]. Alipour *et al*. and Ozcan *et al*. have shown that electrochemically modified PG can be used for detection and determination of morphine and uric acid concentration in blood streams [15,16]. Kara *et al*. have used PG for electrochemical investigation of DNA sequences present in herpes viruses [17]. Several papers have reported the results of comparison between performance of PG and other electrodes with respect to electroanalysis of different compounds [18]. Rubianes *et al.* have compared the performance of several graphite-based electrodes including PG for amperometric determination of dopamine [19]. Several authors have also postulated low background current as one of the most important features of PG [20-22]. Thus, use of PG electrodes for several electroanalytical applications including biosensors, is well known and well established in the literature. Table 1 shows the summary of basic electroanalytical data for few surface modified PG electrodes.

Contrary to biosensors, however, EGBFCs need to produce high potential and current. To enhance the overall performance of EGBFC, enzyme activity and loading need to be improved through several electrode surface modification techniques. Also, the output can be multiplied by cell stacking [3].

Application of PG in EGBFC requires exclusive studies, encouraging thus novel research in this area. In the pioneering work concerning the application of PG in EGBFC, our recent research has already established 5H-grade PG as the optimal biocathode.

(cc) BY

Table 1. *Electroanalytical data of pencil graphite (PG) electrode for various analytes*

PG based electrode	Analyte	Linear range	Detection limit	Ref.
Carmoisine–Cu(II) complex/polyaniline/PG	Cu (II)	5×10^{-6} - 1×10^{-1} M	2×10^{-6} M	[23]
Poly(4-vinyl pyridine)/PG	Cd (II)	1×10^{-7} - 1×10^{-1} M	2.51×10^{-8} M	[24]
Diphenylcarbazide/polyaniline/PG	Cr (IV)	1×10^{-6} - 1×10^{-1} M	8×10^{-7} M	[25]
Platinum nanoparticle/PG	H_2O_2	10 -110 µM	3.6 µM	[26]
Gold nanoparticles/PG	N_2H_4	0.05 -1000 mol L^{-1}	42 nmol L^{-1}	[27]
Gold nanoparticles/PG	Uric acid	0.1- 0.6 mM	-	[28]
Gold nanoparticle/carbon paste/ PG	Glucose	0.0- 33.4 mM	14.2 µM	[29]
Single walled carbon nanotubes /PG	p53 Gene	3.2-8.0 µM	0.88 µM	[30]
Multiwalled carbon nanotubes/PG	Buprenorphine	1.0 - 109.0 pM	0.6 pM	[31]
Gold nanoparticles/chitosan/PG	Deferiprone	0.005-1000 µM	5 nM	[32]
Copper hexacyanoferrate nanostructures (CuHCF/PG)	L-cysteine	1-13 µM	0.13 µM	[33]
SWCNTs-chitosan/PG	Vitamin B12	5.0 - 100.0 nM	0.89 nM	[34]
SWCNTs-chitosan/PG	DNA	10 - 80 µg mL^{-1}	13.2 µg mL^{-1}	[35]
MWCNT/PG	Methadone	0.1- 15 µM	0.087 µM	[36]

In addition, it was shown that PG electrodes of 5H and B grades set as biocathode and bioanode yield the highest full cell performance [37,38]. In continuation of this effort, it would be important to find which PG grade is best suited for bioanode. Accordingly, the objective of the present research work is to evaluate the performance of various grades (H, 3H, 5H and B) of PG in order to identify the grade best suited for bioanode in EGBFC. The surface of these grades of PG were modified first by dip coating of carboxylic acid functionalized multiwalled carbon nanotubes (COOH-MWCNT/PG) and then by covalent immobilization of glucose oxidase (GOx) enzyme, forming GOx/COOH-MWCNT/PG electrode. The relative performances of fabricated PG bioanodes are studied for their efficiency towards oxidation of glucose.

For this study, a mediated electron transfer (MET) is employed using p-benzoquinone as a redox mediator to improve the rate of electron transfer between enzyme and electrode. In anodic enzyme glucose oxidase, the redox active centers are deeply buried in the protein structure making direct electron transfer very difficult [39]. Half-cell and full cell performances of the optimized pencil grade bioanode are evaluated to validate its application to EGBFC.

Experimental

Chemicals

Analytical grade chemicals and materials were procured from Sigma–Aldrich and used as received. They include dibasic sodium phosphate (Na_2HPO_4), monobasic sodium phosphate (NaH_2PO_4), sodium hydroxide (NaOH), hydrogen chloride (HCl), 1-Ethyl-3-(3-dimethylaminopropyl) carbodiimide (EDC), acetone, potassium ferricyanide ($K_3[Fe(CN)_6]$), dimethyl sulfoxide (DMSO), D-(+)-glucose, N-hydroxy succamide (NHS), p-benzoquinone (PBQ), carboxylic acid functionalized multiwalled carbon nanotubes, (COOH-MWCNT) with average diameter and length 9.5 nm and 1.5 µm. Glucose oxidase (GOx) from *Aspergillus niger* was used as biocatalyst for glucose oxidation reaction. It was stored in lyophilized powder at -20 °C. Enzyme solution was freshly prepared before each experiment. Pencil graphite of H, 3H, 5H and B of Apsara brand, India, with 1 cm length and 2 mm diameter, were purchased locally.

Equipment

Electrochemical measurements were performed using Autolab Potentiostat/Galvanostat PGSTAT 302N model (Metrohm, Netherlands) with NOVA 1.11 version software, Biologic model SP-150. The

morphological and elemental composition studies of fabricated PG based bioanodes were performed using scanning electron microscopy performed by Apreo SEM with an energy dispersive X-ray (EDX) instrument.

Procedures

All experiments were carried out at room temperature (25 ± 3 °C) and all solutions were made from milli-Q grade deionized water having specific resistivity 18.2 MΩ cm.

Electrolyte and electrode material

A solution of 0.1 M phosphate buffer was employed as electrolyte for carrying out electrochemical measurements. Appropriate proportions of 0.2 M Na_2HPO_4 and 0.2 M NaH_2PO_4 were added and the pH was fine tuned to 7.0 by either acid (1.0 M HCl) or base (1.0 M NaOH) solutions.

The pencil leads were extracted by peeling the wooden shell using a razor blade. All peeled pencil leads were washed with HCl (0.5 M) for 2 min in ultrasonication bath followed with acetone wash for 2 min using sonicator. The cleaned pencil leads were dried at 90 °C for 2 h in hot air oven to remove moisture content. The pencil leads prepared in this manner were then subjected to surface modification to obtain the pencil graphite electrodes.

Surface modification of PG

Dip coating technique was employed to coat COOH-MWCNT on the surface of cleaned PG. 1.0 mg ml^{-1} dry COOH-MWCNT was added to DMSO and dispersed using a sonicator. The cleaned pencils were dipped in this MWCNT dispersion to ensure proper wetting of PG surface and this was followed by drying to evaporate solvent. For effective adsorption of MWCNT on the surface of PG, the process of wetting followed by drying was repeated four times.

Enzyme immobilization on electrode

Initially, the activation of carboxylic groups was carried out by immersing COOH-MWCNT/PG in EDC/NHS (1:1) solution for 2 h. Thereafter, GOx, the most commonly used enzyme for oxidation of glucose [40], was covalently immobilized on COOH-MWCNT/PG. 7.0 mg of GOx enzyme mixed in 1.0 ml of PBS (0.1 M, pH 7.0) was cast on the surface of COOH-MWCNT/PG and then allowed to dry for 4 h at ambient temperature in proper ventilation. Here, GOx enzyme becomes covalently associated to activated COOH groups in MWCNT by amide bond through bioconjugation technique. Later, the prepared GOx/COOH-MWCNT/PG was rinsed in PBS to remove unattached enzymes.

Electrochemical characterization

Cyclic voltammetry (CV) measurements were performed in three-electrode cell assembly comprising respective grade of GOx/COOH-MWCNT/PG as the working electrode, platinum wire as the counter electrode and Ag/AgCl (sat. KCl) (Metrohm) as the reference electrode. The potential was swept between -0.6 V to 0.6 V (*vs*. Ag/AgCl) with scan rates varied from 10 to 50 mV s^{-1}. It was observed that 10 mV s^{-1} was the optimum scan rate for all tested grades of PG, and therefore, this scan rate was maintained for all experiments. All measurements were made with regard to the geometrical surface area (0.66 cm^2) of prepared bioanodes.

To measure effective electrode surface area (ESA), CV was repeated for the same electrode system in 4 mM $K_3[Fe(CN)_6]$ dissolved in 0.1 M KNO_3 in a voltage range -0.2 – 0.8 V for a series of scan rates ranging from 20 to 100 mV s^{-1} [41].

Electrochemical impedance spectroscopy was performed over the frequency range of 10 kHz to 10 mHz, at an amplitude of 5 mV, resulting in Nyquist plots (-*Z*'' *vs. Z*') of GOx/COOH--MWCNT/PG [42].

(cc) BY

All experiments were repeated with three sets of electrodes fabricated for each grade of pencil graphite to ensure the effectiveness of the fabrication procedure and to evaluate the consistency and reproducibility of the results obtained.

Half-cell and full cell assembly with modified PG bioanode

Half-cell measurements were carried out using a conventional three-electrode system of 25 ml volume capacity comprising the prepared GOx/COOH-MWCNT/PG (modification described above) as the working electrode, platinum wire as the counter electrode and Ag/AgCl (sat. KCl) as the reference electrode. The solution of 0.1 M, pH 7.0 PBS containing 5 mM glucose as redox species was used as the electrolyte. To promote MET, 2 mM p-benzoquinone (PBQ) was added to the electrolyte as a redox mediator [43]. The electrolyte was purged with N_2 gas for 15 min before each experiment to avoid the interference of oxygen to glucose oxidation reaction at anode. Experiments carried out on the said grades of pencils at various scan rates showed that maximum performance was obtained at scan rate of 10 mV s^{-1}. Accordingly, this scan rate was considered as the optimized parameter for carrying out rest of the experiments.

An assembly of enzymatic glucose biofuel cell was used to test GOx/COOH-MWCNT composite modified PG based bioanode using Biologic-150 Potentiostat (Biologic Science instruments, France). EGBFC comprises of 10 ml single compartment membrane-less chamber with GOx/COOH-MWCNT composite modified PG as bioanode and platinum wire as biocathode. The cell is fed with 0.1 M, pH 7.0 PBS containing 5 mM glucose as anodic fuel and ambient air for cathode. PBQ and ABTS were used as anode and cathode redox mediators, respectively.

Any half-cell and full cell set up was configured separately for each tested grade of PG bioanode and the measurements were recorded individually.

Polarization studies were conducted to evaluate the voltage and power output generated by EGBFC. The maximum power output of assembled PG based EGBFC at each known resistance was calculated by multiplying stabilized current and potential. The full cell performance parameters such as current and power densities were calculated based on the geometrical surface area of the electrode. The real images of the experimental set up are shown in Figure 1.

Measurements

Effective surface area of electrode

Effective surface area (ESA) of COOH-MWCNT/PG electrode was evaluated using Randles–Ševčik equation describing the effect of scan rate on peak current in cyclic voltammetry experiments [44]:

$$i_p = 2.69\times10^5 n^{3/2} D^{1/2} C A v^{1/2} \quad (1)$$

In eq. (1), i_p is peak current, n represents the number of electrons transferred during redox reaction, D (cm^2 s^{-1}) represents diffusion coefficient of reaction species, v is the sweep or scan rate (V s^{-1}), C is concentration (M) of reaction species, and A symbolizes the effective surface area of electrode (cm^2). In present experiments, 4 mM $K_3[Fe(CN)_6]$ was applied generating $Fe(CN)_6^{-3}/Fe(CN)_6^{-4}$ redox reaction and D was stated as 6.70×10^{-6} cm^2 s^{-1}.

Peak currents (i_p) were measured at scan rates varying from 20-100 mV s^{-1} using CV and the slope (k) of the obtained linear expression for i_p *vs.* $v^{½}$ was obtained. The slope is then substituted into the following equation to express ESA (A) [41]:

$$A = k/(2.69\times10^5 n^{3/2} D^{1/2}) \quad (2)$$

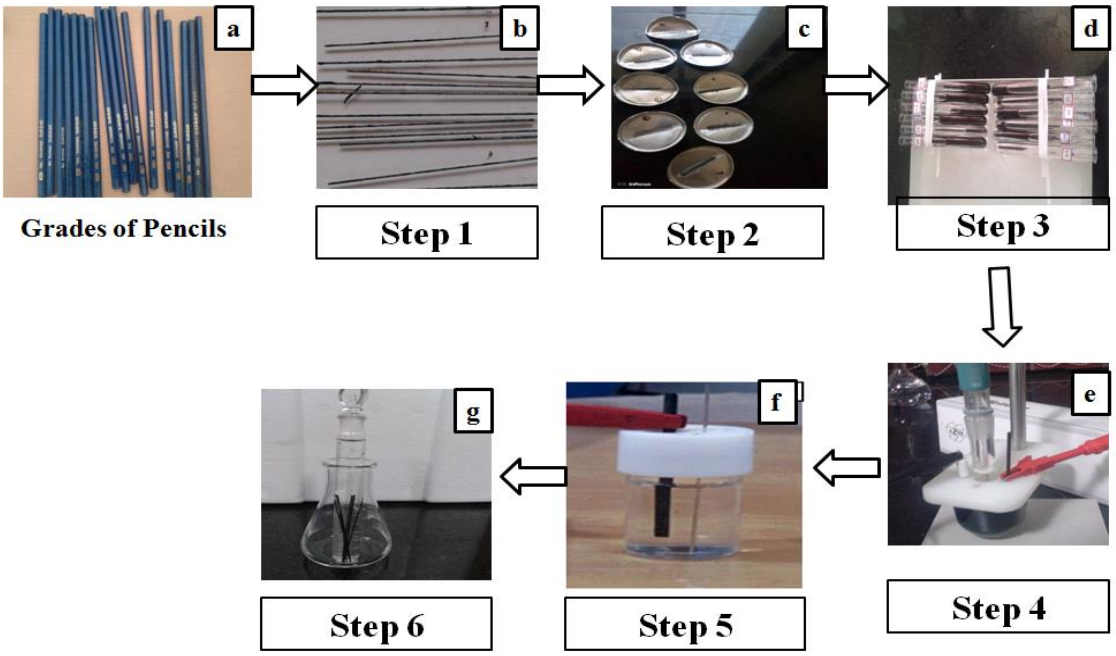

Figure 1. *Real images of stepwise process of PG electrode fabrication: (a) pencil graphite of different grades; (b) peeled and pretreated PG; (c) MWCNT modified PG; (d) enzyme immobilization; (e) PG based bioanode half-cell performance; (f) PG based bioanode full cell EGBFC; (g) storage of fabricated PG bioanode*

Electron transfer kinetics

Electron transfer reaction rate (ETR) constant

The Laviron equation [45] was employed to measure ETR constant (γ) of each grade of fabricated PG based bioanode:

$$\log\gamma = \alpha\log(\alpha-1)+(1-\alpha)\log\alpha-\log\left(\frac{RT}{nFv}\right)-\frac{\alpha(1-\alpha)nF\Delta E_p}{2.3RT} \quad (3)$$

In eq. (3), R stands for gas constant (8.314 J K^{-1} mol^{-1}), v for sweep rate (0.1 V s^{-1}), α is transfer coefficient, T is temperature, K; F is Faraday constant (96485 A s mol^{-1}), n is the number of transferred electrons (n=2) and ΔE_p represents potential difference (V) of cathodic and anodic redox peaks.

Surface enzyme density

The surface concentration of immobilized enzyme in mol cm^{-2} was evaluated using CV measurements and Brown–Anson model [46]:

$$i_p = n^2F^2\Gamma\frac{Av}{4RT} \quad (4)$$

In eq. (4), A represents the electrode geometrical surface area (0.66 cm^2), and Γ stands for the enzyme concentration on MWCNT nanocomposite of the fabricated bioanode surface. Other symbols have their already explained meaning.

Results and discussion

Surface morphology analysis using scanning electron microscope

The structure and morphology of fabricated PG bioanodes (COOH-MWCNT/PG, GOx/COOH-MWCNT/PG) were studied using scanning electron microscopy (SEM). SEM images with 500 nm magnification taken during various stages of fabrication, are shown in Figure 2. Different grades of PG have exhibited different morphological characteristics due to the variation in their composition.

(cc) BY

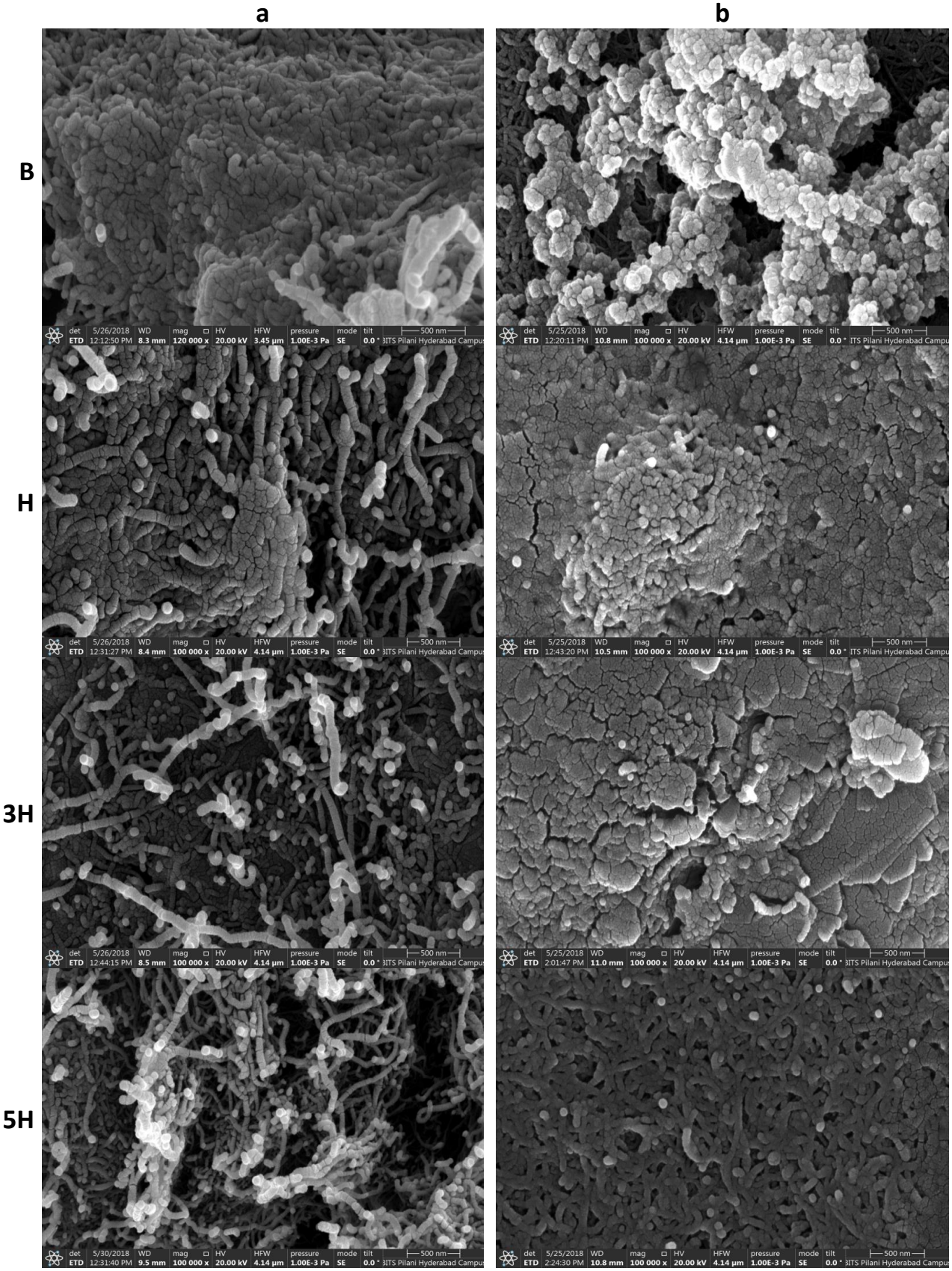

***Figure 2**. SEM micrographs of fabricated (a) COOH-MWCNT/PG and (b) GOx/COOH-MWCNT/PG of B, H, 3H, and 5H grades*

Figure 2a shows SEM images of COOH-MWCNT/PG with a network of MWCNTs distributed on the surfaces of PG of various grades. From SEM images, it can be seen that a relatively high density of MWCNT carpet is observed on B-grade PG when compared to other grades, with noticeably large

quantities of attachment of MWCNT to PG surface. This can be attributed to the porous network structure of B-grade pencil which remains undisturbed by the small amount of binder content. In the case of other grades of pencils, however, the increasing binder content resulted in the blockage of redox sites of the surface functional groups, resulting in sparse deposition as can be seen in SEM images of other PG electrodes. It is assumed that by dip-coating of MWCNT, an increased electrode surface for anchoring of enzymes is provided with improved accessibility of redox species towards immobilized enzymes [47].

Figure 2b shows SEM images of GOx/COOH-MWCNT/PG after GOx immobilization. It is evident that B-grade PG has distinct morphology with relatively high GOx coverage due to greater enzyme loading than at other grades PG. It can be inferred that B-grade PG with its dense deposition of MWCNT matrix with nano-wired structure provides a relatively large surface area that shows affinity towards GOx enzyme, resulting in greater immobilization of GOx on the electrode surface.

Surface morphology analysis using energy dispersive X-ray spectroscopy

In addition to SEM, energy dispersive X-ray spectroscopy (EDX) analysis was employed to confirm the presence of immobilized GOx enzyme on modified PG electrode surface. Figure 3 displays carbon (C) and oxygen (O) contents before and after GOx casting on MWCNT matrix of different grades PG. Before the immobilization of GOx, the unmodified PG showed low oxygen and higher carbon content. After GOx immobilization, however, the oxygen content is increased, and the carbon content reduced. This observation confirms the association of GOx enzyme layer on the surface of modified PG electrode. Relative to other tested grades, higher difference of oxygen and carbon contents before and after GOx immobilization was recorded for B-grade PG, indicating the highest enzyme immobilization among all tested grades of pencils.

It is also evident that the oxygen to carbon ratio for all tested grades of PG is ranging from 13 to 30 % (O/C ratio for B grade PG 13 %), what is close to the O/C ratio of polished glassy carbon electrode (8-15 %) [18].

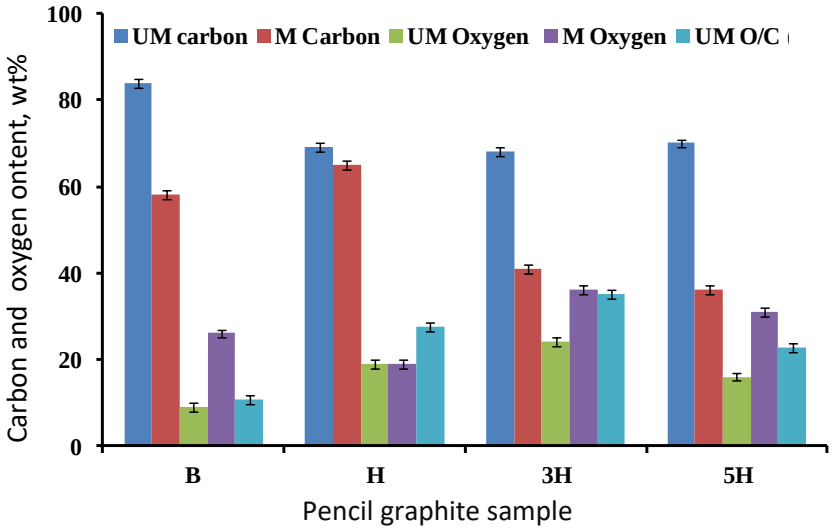

Figure 3. *EDX characterization of carbon and oxygen contents of modified and unmodified PG based bioanode (UM-unmodified; M-modified).*

Electrode characterization using electron transfer kinetics

The electrochemical reduction/oxidation of $[Fe(CN)_6]^{-3}/[Fe(CN)_6]^{-4}$ redox couple was used to compute the kinetics of electron transfer at modified PG electrodes (COOH-MWCNT/PG). The CV

(cc) BY

curves for COOH-MWCNT/PG tested in 4.0 mM $[Fe(CN)_6]^{-3}$ dissolved in 100 mM KNO_3 within the voltage range of -0.2 to 0.8 V at 10 mV s^{-1}, are shown in Figure 4.

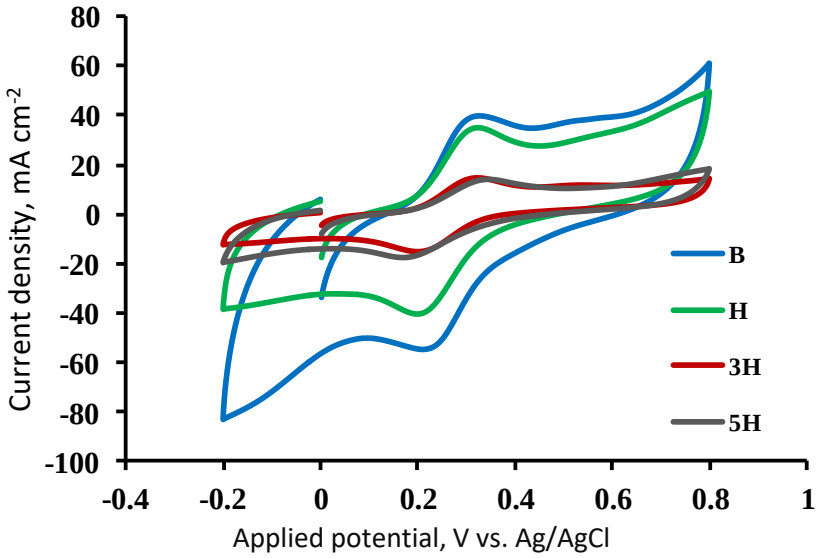

Figure 4. *Cyclic voltammograms for COOH-MWCNT/PG electrode of various grades in 0.1 M KNO_3 containing 4.0 mM $K_3Fe(CN)_6$ at 10 mV s^{-1} scan rate.*

The highest peak currents are observed for B-grade pencil and the ratio of cathodic (i_{pc}) and anodic (i_{pa}) peak currents is close to 1.0, indicating reversible electron transfer kinetics [48]. Also, this grade of PG bioanode showed less anodic and cathodic peak potential difference (ΔE_p) (which is a basis for electrochemical reversibility [46]), indicating that the heterogeneous pseudo reversible electron transfer process is present [40]. The respective peak current densities and ΔE_p values of all tested PG grades are summarized in Table 2.

Effective electrode surface area comparison

Electrochemical reaction of $[Fe(CN)_6]^{-4}/[Fe(CN)_6]^{-3}$ redox couple was also used for evaluation of effective electrode surface area (ESA) of modified PG electrodes (COOH-MWCNT/PG) of various grades. Resulting CV curves of tested COOH-MWCNT/PG electrodes showed well defined redox peaks for the scan rate range 10-100 mVs^{-1} and the linear expression was observed for peak currents plotted *vs.* square root of scan rates. Using Randles–Ševčik equation defined by eq. (1), the values of ESA were calculated using eq. (2) for all grades of COOH-MWCNT/PG and listed in Table 2. The highest ESA was obtained for B-grade COOH-MWCNT/PG, indicating high deposition of MWCNT as can also be observed from SEM images.

Table 2. *Summary of electrochemical parameters for $[Fe(CN)_6]^{-4}/[Fe(CN)_6]^{-3}$ redox reaction at COOH-MWCNT/PG of various grades*

Pencil grade	i_{pa} / µA cm^{-2}	i_{pc}/i_{pa}	ΔE_p / mV	Average value of ESA, cm^2	SD (n=3)	Standard error, % (n=3)
B	1013	1.06	71	0.34	0.01	1
H	968	1.37	100	0.28	0.03	1
3H	896	1.25	103	0.30	0.03	1
5H	900	1.04	152	0.33	0.03	1%

Electrochemical characterization using electrochemical impedance spectroscopy

Electrochemical impedance spectroscopy (EIS) was opted to characterize the interface properties of fabricated PG based bioanodes during their interaction with PBS electrolyte containing 5 mM

glucose. In general, EIS curves reveal semicircles and straight lines at high and low frequencies, respectively. The diameter of the semicircle corresponds to the charge transfer resistance (R_{ct}) of the redox reaction, whilst the straight line represents the superiority of mass diffusion control effect over the charge transfer process [42].

Figure 5 shows electrochemical impedance spectra (Nyquist plots) of GOx/COOH-MWCNT/PG recorded at 0 V *vs*. Ag/AgCl in PBS (0.1 M, pH 7.0) containing 5 mM glucose and 2 mM PBQ as a mediator. It can be observed from impedance spectra in Figure 5 that GOx/COOH-MWCNT/PG electrodes have undergone diffusion controlled redox reaction indicated by straight lines at low frequencies. At high frequencies, however, well defined semicircles corresponding to interfacial charge transfer resistance coupled to double-layer capacitance are noticed for GOx/COOH-MWCNT/PG of all tested grades. The evaluated R_{ct} values are summarized in Table 3, showing variations between 2 to 8 Ω cm^2. It can also be inferred that B-grade GOx/COOH-MWCNT/PG offered the lowest resistance to electron transfer among all tested PG bioanodes. This may be attributed to the deposition of dense conducting matrix of MWCNT on PG surface. Larger value of R_{ct} for 3H-grade PG may be due to large amount of clay content, as also seen by EDX analysis, which offers more resistance for electron transfer.

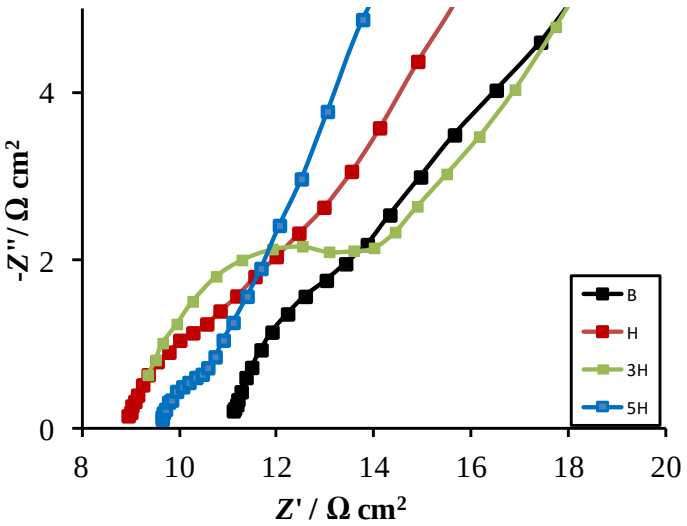

Figure 5. *Nyquist plots of GOx/COOH-MWCNT/PG bioanodes fabricated from various grades of PG in 0.1 M pH 7.0 PBS containing 5 mM glucose and 2 mM PBQ. Frequency range: 10 kHz -10 mHz; Amplitude: 5 mV*

Electrochemical characterization of GOx/COOH-MWCNT/PG electrodes using CV

Biocatalytic activity

The biocatalytic activity of GOx/COOH-MWCNT/PG based bioanodes towards glucose oxidation was also tested using CV. All the experiments were carried out in N_2 gas saturated 0.1 M, pH 7.0 PBS containing 5 mM glucose at the sweep rate of 10 mVs^{-1}. The resulting CV curves are presented in Figure 6, showing well defined oxidation peaks at potentials between 200 to 300 mV for all grades of PG bioanodes. Varying current densities are observed with the highest peak current density of 4.25 mA cm^{-2} recorded at peak potential of 253 mV for B-grade bioanode. This may be due to the enhanced surface area attained by increasing amount of MWCNT deposition as can be seen from SEM images and high graphite content [18].

(cc) BY

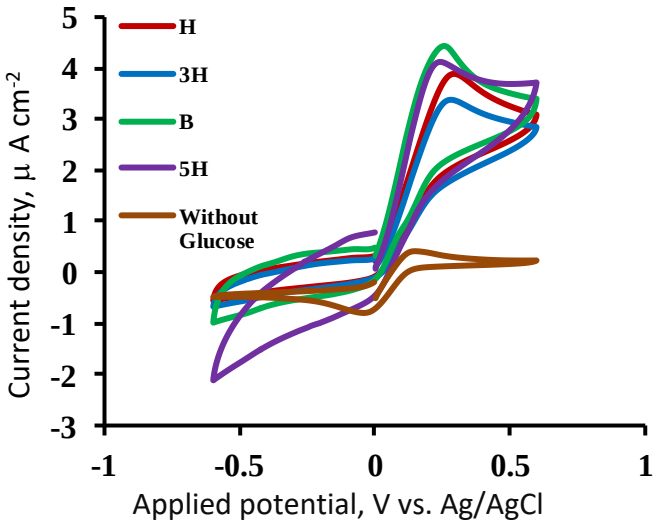

Figure 6. *CVs of GOx/COOH-MWCNT/PG bioanodes of different grades in 0.1 M PBS pH 7.0, containing 5 mM glucose, recorded at 10 mVs^{-1}.*

Immobilized GOx enzyme kinetics

Using the same CV studies, anodic peak currents were plotted against a series of scan rates for each fabricated PG bioanode. A linear raise in anodic peak current with increase in sweep rate was observed. Using Laviron (eq. (3)) and Brown–Anson equation (eq. (4)), the electron transfer rate (ETR) constant (γ) and surface concentration (Γ) of deposited nanobiocomposite for all tested PGs were determined and listed in Table 3. The values of ETR constants for all tested grades of pencil leads are varied from 2.0 to 5.4 s^{-1}, and the highest surface concentration of enzymes biocomposite is observed for B-grade bioanode showing the fastest ETR (5.39 s^{-1}), what agrees with SEM results.

Table 3. *Electrochemical characteristics of GOx/COOH-MWCNT/PG bioanodes*

Pencil grade	R_{ct} / Ω cm^2	i_{pa} / μAcm^{-2}	γ / s^{-1}	Γ / mol cm^{-2}×10^{-10}
B	2	4250	5.39	2.42
H	5	163	1.96	1.79
3H	8	3086	2.62	1.82
5H	3	3910	3.87	2.27

Biofuel cell performance of GOx/COOH-MWCNT modified PG bioanode

To validate the application of fabricated bioanodes for EGBFC, a prototype membrane-less enzymatic glucose biofuel cell was assembled using GOx/COOH-MWCNT/PG as bioanode and platinum wire as cathode. Both electrodes were immersed in PBS (0.1 M, pH 7.0) contained in 10 ml beaker at atmospheric conditions. Figure 7a shows the real image of assembled membrane-less enzymatic glucose biofuel cell. It can be clearly observed from Figure 7a, that PG-based bioanode of B-grade in PBS (0.1 M, pH 7.0) containing 5 mM glucose is well-suited for further miniaturization. Figure 7b presents current density (*I*) and power density (*P*) of EGBFC (*I vs*. *P* and *I vs. V* curves) as a function of operation cell voltage taken at room temperature (25 ± 3°C). The current density was calculated with respect to the electrochemical active surface area (ESA) of bioanode. Figure 7b shows that open circuit potential (OCP) and maximum current density of EGBFC are 149 ± 3 mV and 38 ± 0.7 μA cm^{-2}, respectively. Further, a maximum power density of 0.789 μW cm^{-2} can be attained at 141 mV. This value is very close to that of anodes made from carbon cloth [49,50] and even greater than those of anodes based on reduced graphene oxide (rGO/MWCNT) based carbon [51]. This proves the applicability of the fabricated bioanode to EGBFC. At the same time, the value of

maximum power density is somewhat smaller than for carbon or MWCNT based wired enzyme bioanodes [52-54]. However, the unique advantages of PG like low cost, quick surface renewal and ease of modification and miniaturization, off-set its lower performance levels, maintaining thus applicability of PG to miniaturized bioelectronic systems.

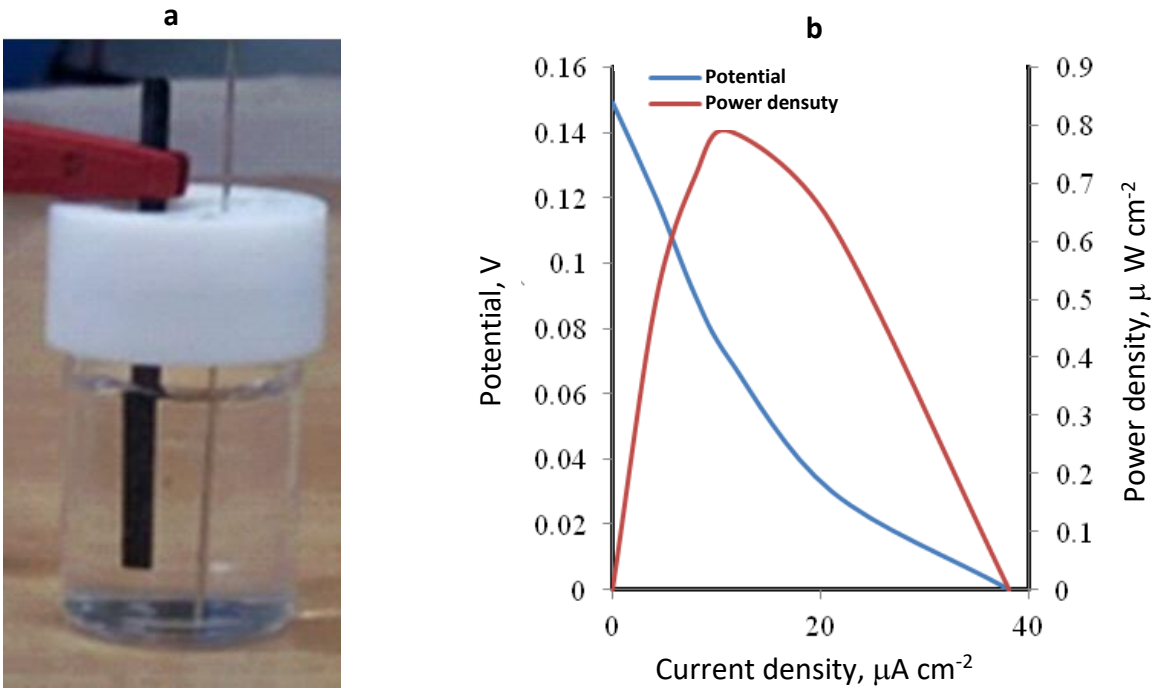

Figure 7. *a) Real image of the assembled single chamber membrane-less EGBFC with an optimized grade PG as bioanode and platinum wire as biocathode in contact with 5 mM glucose dissolved in 0.1 M, pH 7.0 PBS containing 3 mM ABTS and 3 mM PBQ as anodic and cathodic mediators and under air saturated conditions. b) Potential and power density vs. current density plots of EGBFC containing optimized PG bioanode obtained by polarization studies at 25 ± 3 °C.*

Conclusions

This work demonstrates the application of modified pencil graphite (PG) of different grades as suitable bioanodes for enzymatic glucose biofuel cell (EGBFC). Morphological characterization of tested PG of grades H, 3H, 5H, and B have indicated some variations in enzyme immobilization on the surface of PG, based on their composition and surface structure. The tested PG bioanodes exhibited positive responses towards glucose oxidation reaction with the fastest electron transfer rate recorded for B-grade PG. The half-cell assembly with this PG grade bioanode showed the highest current density of 4.25 mA cm^{-2} under physiological glucose concentration conditions. The obtained results reveal that physical and electrochemical characteristics of B-grade PG bioanode are comparable to those of conventional carbon and glassy carbon electrode substrates.

The membrane-less enzymatic glucose biofuel cell assembled with B-grade PG bioanode showed OCP at 149 mV, maximum power density of 0.789 μW cm^{-2} and current density of 38 ± 0.7 μA cm^{-2} at 141 mV voltage, respectively. Since these values are very close to those of anodes made from carbon cloth modified with MWCNT and even greater than those of anodes based on rGO/MWCNT based carbon, the applicability of the fabricated bioanode to EGBFC becomes clear.

The performance can be further optimized by subjecting PG to additional surface modifications with nanomaterials and conductive polymers. Alternate enzyme immobilizing techniques can also be explored to enhance enzyme reaction kinetics. The performance is also likely to vary by introduction of PG based biocathode to realize fully assembled EGBFC using PG electrodes. Once

(cc) BY

optimized, a lab scale membrane-less EGBFC would be assembled with the optimized PG as bioanode and biocathode with laccase and glucose oxidase enzymes. Evaluating the performance of EGBFC assembled with the optimized grade PG electrodes will give further insights into possible practical real time applications.

References

[1] D. Kashyap, P. S. Venkateswaran, P. K. Dwivedi, YH. Kim, GM. Kim, A. Sharma, S. Goel, *International Journal of Nanoparticles* **8** (2015) 61-81.
[2] J. Kim, H. Jia, P. Wang, *Biotechnology Advances* **24** (2006) 296-308.
[3] M. Holzinger, A. Le Goff, S. Cosnier, *Electrochimica Acta* **82** (2012) 179-190
[4] J. M. Friedrich, C. Ponce-de-León, G. W. Reade, F. C. Walsh, *Journal of Electroanalytical Chemistry* **561** (2004) 203-217.
[5] A. K. Sarma, P. Vatsyayan. P. Goswami, S. D. Minteer, *Biosensors and Bioelectronics* **24** (2006) 2313-2322.
[6] K. Aoki, T. Okamoto, H. Kaneko, K. Nozaki, A. Negishi, *Journal of Electroanalytical Chemistry and Interfacial Electrochemistry* **263** (1989) 323-331.
[7] *I. G. David, D. E. Popa, M. Buleandra, Journal of Analytical Methods in Chemistry* (2017) Article ID 1905968 https://doi.org/10.1155/2017/1905968
[8] J. K. Kariuki, *Journal of the Electrochemical Society* **159** (2012) 747-751.
[9] P. H. C. P. Tavare, P. J. S. Barbeira, *Journal of Applied Electrochemistry* **38** (2008) 827-832.
[10] E. Alipour, M. R. Majidi, A. Saadatirad, S. M. Golabi, A. M. Alizadeh, *Electrochimica Acta* **91** (2103) 36-42.
[11] Z. Q. Gong, A. N. Sujari, S. Ab Gha*ni, Electrochimica A**cta* **65** (2012) 257-265.
[12] L. Liv, N. Nakiboglu, *Turkish Journal of Chemistry* **40** (2016) 412-421.
[13] J. Wang, A. N. Kawde, E. Sahlin, *Analyst* **125** (2000) 5-7.
[14] J. Wang, A. N. Kawde, *Analytica Chimica Acta* **413** (2001) 219-224.
[15] E. Alipour, S. Gasemlou, *Analytical Methods* **4** (2012) 2962-2969.
[16] A. Ozcan, Y. Sahin, *Biosensors and Bioelectronics* **25** (2010) 2497-2502.
[17] P. Kara, B. Meric, A. Zeytinoglu, M. Ozsoz, *Analytica Chimica Acta* **518** (2004) 69-76.
[18] A. M. Bond, P. J. Mahon, J. Schiewe, V. Vicente-Beckett, *Analytica Chimica Acta* **345** (1997) 67-74.
[19] M. D. Rubianes, G. A. Rivas, *Analytical Letters* **36** (2003) 329-345.
[20] S. Buratti, M. Scampicchio, G. Giovanelli, S. Mannino, *Talanta* **75** (2008) 312-316.
[21] A. N. Kawde, N. Baig, M. Sajid, *RSC Advances* **6** (2016) 91325-40.
[22] M. R. Akanda, M. Sohail, M. A. Aziz, A. N. Kawde, *Electroanalysis* **28** (2016) 408-424.
[23] R. Ansari, A. F. Delavar, A. Aliakbar, A. Mohammad-Khah, *Journal of Solid State Electrochemistry* **16** (2012) 869-875.
[24] J. L. Ling, *A. Khan, B. Saad, S. Ab Ghani, Talanta* **88** (2012) 477-483.
[25] M. K. Ali, R. Ansari, A. F. Delavar, Z. Mosayebzadeh, *Bulletin of the Korean Chemical Society* **33** (2012) 1247-1252.
[26] A. N. Kawde, M. Aziz, N. Baig, Y. Temerk, *Journal of Electroanalytical Chemistry* **740** (2015) 68-74.
[27] M. A. Aziz, A. N. Kawde, *Talanta* **115** (2013) 214-221.
[28] H.C. Kalachar**,** Y.A. Naik, *International Journal of Chem Tech Research* **3** (2011) 1237-1245.
[29] C. Cheng, K.C. Chang, C.S. Chena, D.G. Pijanowska, *Journal of Chinese Chemical Society* **58** (2011) 739-748.
[30] G. Congur, M. Plucnara, A. Erdem, M. Fojta, *Electroanalysis* **27** (2015) 1579-1586.
[31] A.A. Ensafi, E. Khoddami, B. Rezaei, *Talanta* **116** (2013) 1113-1120.
[32] J. Narang, N. Malhotra, G. Singh, C.S. Pundir, *Biosensors and Bioelectronics* **66** (2015) 332-337.
[33] M. R. Majidi, K. Asadpour-Zeynali, B. Hafezi, *Microchimica Acta* **169** (2010) 283-288.
[34] F. Kuralay, T. Vural, C. Bayram, E.B. Denkbas, S. Abaci, *Colloids and Surfaces B: Biointerfaces* **87** (2011) 18-22.
[35] A. Erdem, M. Muti, H. Karadeniz, G. Congur, E. Canavar, *Colloids and Surfac**es** B: Biointerfaces* **95** (2012) 222-228.
[36] E. Alipour, M.R. Majidi, O. Hoseindokht, *Journal of Chinese Chemical Society* **62** (2015) 461-468.

[37] M**.** Bandapati, P.K. Dwivedi, B. Krishnamurthy*, Y.* H. Kim, G. M. Kim, S. Goel, *International Journal of Hydrogen Energy* **42** (2017) 27220-27229.
[38] M. Bandapati, B. Krishnamurthy, S. Goel, *IEEE Transactions on Nanobioscience* **18** (2) (2019) 170-175.
[39] K. Ahmad, M. Naushad, *International Journal of Hydrogen Energy* **39** (2014) 7417-7421.
[40] D. Ivnitski, B. Branch, P. Atanassov, C. Apblett, *Electrochemical Communication* **8** (2016) 1204-1210.
[41] J. Shi, J. C. Claussen, E.S. McLamore, A. ul Haque, D. Jaroch, A.R. Diggs, P. Calvo-Marzal, J. L. Rickus, D.M. Porterfield, *Nanotechnology* **22(35)** (2011) 355502.
[42] D. Kashyap, P.K. Dwivedi, J.K. Pandey, Y.H. Kim, G.M. Kim, A. Sharma, S. Goel, *International Journal of Hydrogen Energy* **39** (2014) 20159-170.
[43] T. Ikeda, I. Katasho, M. Kamei, M. Senda, *Agricultural and Biological Chemistry* **48** (1984) 1969-1976.
[44] A. J. Bard, L.R. Faulkner, *Electrochemical Methods: Fundamentals and Applications*, Wiley, 2000.
[45] E. Laviron, *Journal of Electroanalytical Chemistry and Interfacial Electrochemistry* **10** (1979) 19-28.
[46] A. P. Brown, F. C. Anson, *Analytical Chemistry* **11** (1977)1589-1595.
[47] F. Lopez, S. Zerria, A. Ruff, W. Schuhmann, *Electroanalysis* **7** (1977) 1311-1318.
[48] K. Gong, M. Zhang, Y. Yan, L. Su, L. Mao, S. Xiong, Y. Chen, *Analytical Chemistry* **76** (2005) 6500-5.
[49] B. C. Kim, I. Lee, S. J. Kwon, Y. Wee, K.Y. Kwon, C. Jeon, H. J. An, H. T. Jung, S. Ha, J. S. Dordick, J. Kim, *Scientific Reports* **7** (2017) 40202.
[50] M. Ammam, J. Fransaer, *Biotechnology and Bioengineering* **109** (2012) 1601-1609.
[51] S. Palanisamy, S. Cheemalapati, S. M. Chen, *International Journal of Electrochemical Science* **11** (2012) 11477-87.
[52] Y. Li, S. M. Chen, R. Saraswathi, *International Journal of Electrochemical Science* **6** (2011) 3776-3788.
[53] R. Haddad, W. Xia, D. A. Guschin, S. Pöller, M. Shao, J. Vivekananthan, M. Muhler, W. Schuhmann, *Electroanalysis* **25** (2013) 59-67.
[54] A. Kumar, S. Sharma, L. M. Pandey, P. Chandra, *Materials Science for Energy Technologies* **1** (2018) 38-48.

©2020 by the authors; licensee IAPC, Zagreb, Croatia. This article is an open-access article distributed under the terms and conditions of the Creative Commons Attribution license (http://creativecommons. org/licenses/by/4.0/)